

Measuring Supermassive Black Holes in Distant Galaxies with Central Lensed Images

David Rusin¹, Charles R. Keeton², Joshua N. Winn^{3,4}

ABSTRACT

The supermassive black hole at the center of a distant galaxy can be weighed, in rare but realistic cases, when the galaxy acts as a strong gravitational lens. The central image that should be produced by the lens is either destroyed or accompanied by a second central image, depending on the mass of the black hole. We demonstrate that when a central image pair is detected, the mass of the black hole can be determined with an accuracy of $\lesssim 0.1$ dex, if the form of the smooth mass distribution near the galaxy core is known. Uncertainty in the central mass distribution introduces a systematic error in the black hole mass measurement. However, even with nearly complete ignorance of the inner mass distribution, the black hole mass can still be determined to within a factor of 10. Central image pairs should be readily observable with future radio interferometers, allowing this technique to be used for a census of supermassive black holes in inactive galaxies at significant redshift ($0.2 \lesssim z \lesssim 1.0$).

Subject headings: galaxies: nuclei—black hole physics—gravitational lensing

1. Introduction

Supermassive black holes (SMBHs) reside at the centers of most galaxies, and are the power sources for active galactic nuclei (AGNs). For nearby galaxies, empirical correlations have been discovered between the mass of the SMBH and various galactic properties such as the bulge mass (Laor 2001), velocity dispersion (Ferrarese & Merritt 2000; Gebhardt et al. 2000; Tremaine et al. 2002), luminosity (Magorrian et al. 1998; McLure & Dunlop 2001, 2002), and concentration (Graham et al. 2001). The existence of these correlations suggests a relationship between black hole growth and galaxy formation (e.g., Kauffmann & Haehnelt 2000; Monaco et al. 2000; Wyithe & Loeb 2002; Haiman et al. 2004).

An important step forward would be to trace the evolution of these correlations over cosmic time (see, e.g., Treu et al. 2004; Robertson et al. 2005). For this, we need a way to measure

¹Department of Physics & Astronomy, University of Pennsylvania, 209 So. 33rd St., Philadelphia, PA 19104-6396

²Department of Physics & Astronomy, Rutgers University, 136 Frelinghuysen Road, Piscataway, NJ 08854

³Harvard-Smithsonian Center for Astrophysics, 60 Garden St., Cambridge, MA 02138

⁴Hubble Fellow

central black hole masses in galaxies at significant redshift. Two techniques have provided most of the existing black hole mass measurements. First, in normal galaxies, the SMBH mass can be determined from the kinematics of stars or gas near the galaxy center (Magorrian et al. 1998; Gebhardt et al. 2003). Although this method offers very accurate masses, it requires spectroscopy with high spatial resolution, which can only be achieved for nearby galaxies. Second, in reverberation mapping of active galaxies (Blandford & McKee 1982; Kaspi et al. 2000; Peterson et al. 2004), the orbital parameters of gas clouds can be estimated from the width of the broad emission lines and the time lag between continuum and line variability, yielding a measurement of the SMBH mass. This method works at higher redshift, but it cannot be applied to normal, quiescent galaxies.

Gravitational lensing supplements these techniques by offering a way to detect and measure SMBHs in ordinary galaxies at intermediate redshift ($0.2 \lesssim z \lesssim 1.0$). The starting point is the generic prediction that the multiple lensed images of a background object should include a faint image that appears close to the center of the lens (Burke 1981). A SMBH in the lens galaxy will alter the properties of this image, in one of two ways (Mao et al. 2001). For certain SMBH masses and source positions, the black hole destroys the central image. If that does not happen, then the SMBH creates an *additional* image.

Radio observations seem to be the likeliest route to finding central images, because of the necessary angular resolution and dynamic range, and because dust extinction is not a problem at radio wavelengths. Bowman et al. (2004) recently calculated the probability of finding central image pairs produced by a SMBH, and concluded that the next generation of radio telescopes is needed to discover them in large numbers. In this Letter, we investigate what will be learned when a central image pair is detected: namely, with what accuracy can the mass of the SMBH be measured? The issue is timely because the best candidate for a central image has recently been found in the lens system PMN J1632–0033 (Winn et al. 2003b, 2004). Since the central image has apparently not been destroyed in that system, there must be a faint companion image if the lens galaxy hosts a SMBH.

Section 2 reviews the phenomenology of central images. Section 3 presents an analysis of simulated central image systems, and § 4 summarizes and discusses these results. Standard values for the cosmological parameters ($\Omega_m = 0.3$, $\Omega_\Lambda = 0.7$, and $H_0 = 65 \text{ km s}^{-1} \text{ Mpc}^{-1}$) are assumed for all calculations.

2. The Phenomenology of Central Images

In the language of lensing theory (see, e.g., Kochanek et al. 2004), the formation of a central image requires the existence of a radial critical curve. For spherical models, this is equivalent to a solution of the equation $d\alpha(R)/dR = 1$, where $\alpha(R)$ is the deflection angle and R is the image-plane radius. Many commonly used mass models have exactly one solution, such as the nonsingular isothermal sphere (NIS), and single or broken power-law profiles with an inner slope

that is shallower than isothermal ($\rho \propto r^{-\beta}$ with $\beta < 2$). These models produce one central image, and have been described in detail by Wallington & Narayan (1993), Rusin & Ma (2001) and Keeton (2003).

As an example, Figure 1 shows the deflection profile of the NIS model, which produces three images of any source within the radial caustic. We denote these images as A (minimum), B (saddle point) and C (maximum).¹ The addition of a compact mass at the lens center modifies the properties of central images because it causes the deflection angle to diverge as $R \rightarrow 0$, creating a second radial critical curve. Consequently, a sufficiently misaligned source ($R_{s,1}$) produces a second central image: a saddle point, denoted as D. In contrast, no central images form if the source is well aligned ($R_{s,2}$). This illustrates the general conclusion that the SMBH either destroys the central image, or introduces a second one (Mao et al. 2001).

For a given profile, detectable central image pairs only form over a narrow range of black hole masses. We illustrate this by considering a spherical power-law (PL, $\rho \propto r^{-\beta}$) galaxy with a SMBH at $z = 0.5$, and a source at $z = 1.5$. The models are normalized to a typical Einstein radius of $0''.75$. Our definition of “detectable” is $\mu_C/\mu_A > 2 \times 10^{-3}$ and $\mu_D/\mu_C > 10^{-2}$, where μ is the magnification. This is intended to simulate a realistic survey in which systems with a maximum-time image are sought first, and then followed up with more sensitive observations to detect the additional saddle-point image.

In Figure 2 we plot the fractional area within the radial caustic that produces detectable central images, as a function of M_{BH} .² For each choice of β , detectable central images form over a range of M_{BH} spanning less than one decade. The high-mass cutoff occurs where the SMBH destroys the central images, a threshold that is independent of the detectability criteria. The low-mass cutoff, in contrast, is enforced by the lower bounds on μ_C/μ_A and μ_D/μ_C . Thus, smaller black holes could be detected with more sensitive observations.

The mass range that produces central image pairs is (fortuitously) coincident with astrophysically realistic SMBHs. Using an isothermal approximation to relate the image separation to the velocity dispersion, we find that the local $M_{BH}-\sigma$ relation (Tremaine et al. 2002) predicts that a SMBH of mass $\log(M_{BH}/M_{\odot}) = 8.2 \pm 0.2$ will reside in our example galaxy – well within the detectable range for most mass profiles (Fig. 2).

¹The terminology indicates whether the image forms at a minimum, saddle point, or maximum in the time delay surface (Schneider 1985, Blandford & Narayan 1986).

²The results can be generalized to any Einstein radius, black hole mass, cosmology and redshifts by noting that they depend only on the ratio M_{BH}/M_{Ein} , where M_{Ein} is the projected mass within the Einstein radius.

3. Monte Carlo Simulations

Next we turn to the question of how accurately the mass of the SMBH can be recovered from observations of a central image pair. Because a pair of central images has yet to be detected in any real lens system, our answer must rely upon simulations.

We create simulated lenses using a PL model with an Einstein radius of $0''.75$, a central point mass, and an external shear of 10%. We consider profiles spanning the range $1.75 \leq \beta \leq 1.95$, which is consistent with many observed lens galaxies (see, e.g., Rusin et al. 2003; Winn et al. 2003b; Treu & Koopmans 2004; Rusin & Kochanek 2005), and produces detectable central image pairs with reasonable probability. For each β we focus on the range of M_{BH} that is most efficient at creating such systems (Fig. 2). We focus exclusively on “doubles” (which have two bright images and two faint central images) because they generally produce much brighter central images than “quads” (Mao et al. 2001, Keeton 2003). We perturb the simulated lens data using Gaussian errors of 1 mas for the image positions (typical of radio observations), 20% for the fluxes (typical of systematic errors due to mass substructure or microlensing), and 20 mas for the lens galaxy position.

We re-fit the simulated lenses using models consisting of a spherical galaxy, a central point mass, and an external shear field. The models have 4 degrees of freedom. We simultaneously optimize all parameters using a standard χ^2 statistic including contributions from the image positions and magnifications, and lens galaxy position. For an ensemble of lenses created from a given set of input parameters, we extract the distribution of best-fit values of $\log M_{BH}$, which we describe by its mean and standard deviation. For each individual lens we also calculate the range of acceptable $\log M_{BH}$ using the $\Delta\chi^2$ method, verifying that these uncertainties correspond closely to the standard deviation of the ensemble.

First we re-fit the simulated lenses using the parent PL model. We find that the input black hole mass can be recovered with an accuracy of 0.05 – 0.10 dex in M_{BH} . This excellent accuracy is related to the very tight simultaneous constraint that we derive on the logarithmic density slope β . As modeling of the three-image lens PMN J1632–0033 has shown, the properties of image C are sufficient to constrain the PL slope (Winn et al. 2003b). The properties of image D then determine M_{BH} .

The preceding results assume that the functional form of the galaxy mass distribution is known. In reality, uncertainty in the central mass profile can lead to a systematic error. To investigate this error, we re-fit the simulated lenses with a NIS profile instead of a PL profile. These two models are qualitatively different in the inner region where central images form, yet the lensing data alone may not be able to discriminate between them (Winn et al. 2003b). We find that a pair of central images does no better than a single central image in distinguishing between PL and NIS galaxies. Furthermore, the NIS model yields black hole masses that are systematically larger than the “true” (PL) values. Figure 3 shows the systematic offset at a single input M_{BH} for different input β . The

offset is 0.6 dex for $\beta = 1.75$, and increases to 1.0 dex at $\beta = 1.95$.³ For the PL slope that best fits PMN J1632–0033 ($\beta = 1.90$), the offset is 0.8 dex.

We believe that the PL versus NIS analysis gives an upper bound on the systematic error in M_{BH} , because there is a finite range of inner slopes for a realistic galaxy, and the PL and NIS models bracket this range. First, the NIS model has the shallowest possible inner profile (a finite-density core) because the density is expected to decrease monotonically with radius. Second, galaxy mass profiles are always observed to become shallower at smaller radius, rather than steeper (Byun et al. 1996; Ravindranath et al. 2001; Trujillo et al. 2004). Hence the inner profile is not steeper than the best-fit global power-law profile.

To show explicitly that the systematic error depends mainly upon the inner logarithmic slope of the mass distribution, we next consider a broken power-law (BPL) model, for which the surface density varies as $R^{-\gamma_{in}}$ for $R < R_0$, and as $R^{-\gamma_{out}}$ for $R \geq R_0$. By fixing the outer slope at the isothermal value ($\gamma_{out} = 1$), the BPL can approximate both the NIS (for $\gamma_{in} = 0$) and the PL (for $R_0 \rightarrow \infty$, $\gamma_{in} = \beta - 1$). In Figure 4 we show the results of fitting the BPL model to simulated lenses generated with a PL model.

The BPL analysis yields three main results. First, as before, we find that it is not possible to distinguish among different values of γ_{in} . Second, we find that the recovered $\log M_{BH}$ varies systematically with γ_{in} , bridging the PL and NIS limits. Third, we find that the inferred $\log M_{BH}$ varies less strongly with γ_{in} when that slope is shallow, as opposed to steep. Most of the variation in $\log M_{BH}$ occurs just as the model is reaching the PL limit. Thus, even a crude determination of γ_{in} from other observations should substantially reduce the systematic error. Empirically, Byun et al. (1996) and Ravindranath et al. (2001) found that the majority of nearby ellipticals have inner luminosity profiles with $\gamma_{in} < 0.6$.

Can additional constraints help to differentiate among galaxy models? We investigated three ideas: (1) a high-precision (1 mas) measurement of the galaxy center, as might be available if the SMBH acts as an AGN; (2) well-measured time delays (~ 0.5 day) among all images; and (3) a requirement that the mass quadrupole be aligned with the observed position angle of the lens galaxy to within 20° (see, e.g., Kochanek 2002; Winn et al. 2003a). Unfortunately, our simulations show that these constraints, even in combination, do not break the degeneracy between the inner density profile and M_{BH} . The time delays among B, C and D are typically too short to be useful, and the shear constraint adds little information. Most promising is the constraint on the black hole position, which in some cases can distinguish between the PL and NIS models at the 2–3 σ level. Of course, it is not necessarily true that the AGN precisely marks the center of the galaxy mass distribution.

³The offset rises very rapidly as $\beta \rightarrow 2$. For example, the systematic error is 1.4 dex at $\beta = 1.98$, up from 1.0 dex at $\beta = 1.95$. This is of little concern, however, as the cross section for producing detectable central image pairs is very small for $\beta > 1.95$.

4. Summary and Discussion

We have investigated the power of a central image pair to measure the mass of a SMBH. By creating and modeling simulated lens systems, we draw two main conclusions. First, if we know the form of the galaxy mass distribution over the range of radii where central images appear, then realistic observations will determine M_{BH} to within 0.1 dex. Second, uncertainty in the inner mass distribution introduces a significant systematic error in M_{BH} . Our simulated lens data were fitted equally well with a power law (PL) and a nonsingular isothermal sphere (NIS), but the inferred values of M_{BH} were 0.6–1.0 dex larger for the NIS fit. On physical and empirical grounds, we believe that this is the maximum systematic error in M_{BH} . We also explicitly demonstrated the dependence of M_{BH} on the inner profile slope, using a broken power-law (BPL) model.

Despite the systematic error, we believe that the lensing technique will be useful. We are not aware of any other proposed method for the direct measurement of black hole masses in distant, inactive galaxies. Furthermore, we note that the maximum systematic error for SMBHs at *intermediate redshift* is only 2–3 times larger than the statistical error in *local* black hole measurements. The systematic error could be eliminated by directly measuring the inner luminosity (and hence mass) profile of the lens galaxy, although this will be very difficult. An alternative would be to apply priors based on observations of local ellipticals.

Apart from the high sensitivity needed to detect central image pairs, there are additional observational challenges. First, one must rely on the usual lens tests – a common spectrum, surface brightness, and correlated variability – to show that a radio source is actually a central image rather than an AGN in the lens galaxy. Second, high-frequency observations may be required to minimize the effects of free-free absorption (Winn et al. 2003b). Finally, stellar microlensing and halo substructure can perturb the magnifications of central images, complicating the interpretation of measured flux densities. Such effects, however, are not expected to significantly degrade the accuracy of the method, mainly because of the large angular size of the background radio source (G. Dobler et al., in preparation).

Future observations with the Square Kilometer Array offer the best hope for overcoming these issues and discovering large samples of lenses with central image pairs. Since the outer images reveal the galaxy mass, and the central image pairs determine the black hole mass, this instrument may allow us to investigate the evolution of the black hole–galaxy connection.

We thank Avi Loeb, Chris Kochanek, and Greg Dobler for helpful discussions. Work by J.N.W. was supported by NASA through Hubble Fellowship grant HST-HF-01180.02-A, awarded by the Space Telescope Science Institute, which is operated by the Association of Universities for Research in Astronomy, Inc., for NASA, under contract NAS 5-26555.

REFERENCES

- Blandford, R., & McKee, C.F. 1982, *ApJ*, 255, 419
- Blandford, R., & Narayan, R. 1986, *ApJ*, 310, 568
- Bowman, J.D., Hewitt, J.N., & Kiger, J.R. 2004, *ApJ*, 617, 81
- Burke, W.L. 1981, *ApJL*, 244, L1
- Byun, Y.-I., Grillmair, C.J., Faber, S.M., Ajhar, E.A., Dressler, A., Kormendy, J., Lauer, T.R., Richstone, D., & Tremaine, S. 1996, *AJ*, 111, 1889
- Ferrarese, L., & Merritt, D. 2000, *ApJL*, 539, L9
- Gebhardt, K., et al. 2000, *ApJL*, 539, L13
- Gebhardt, K., et al. 2003, *ApJ*, 583, 92
- Graham, A.W., Erwin, P., Caon, N., & Trujillo, I. 2001, *ApJL*, 563, L11
- Haiman, Z., Ciotti, L., & Ostriker, J.P. 2004, *ApJ*, 606, 763
- Kaspi, S., Smith, P.S., Netzer, H., Maoz, D., Jannuzi, B.T., & Giveon, U. 2000, *ApJ*, 533, 631
- Kauffmann, G., & Haehnelt, M. 2000, *MNRAS*, 311, 576
- Keeton, C.R. 2003, *ApJ*, 582, 17
- Kochanek, C.S. 2002, in *Proceedings of the Yale Cosmology Workshop: The Shapes of Galaxies and Their Dark Matter Halos*, P. Natarajan, ed. (Singapore: World Scientific)
- Kochanek, C.S., Schneider, P., & Wambsganss, J. 2004, Part 2 of *Gravitational Lensing: Strong, Weak & Micro*, *Proceedings of the 33rd Saas-Fee Advanced Course*, G. Meylan, P. Jetzer & P. North, eds. (Berlin: Springer-Verlag) (astro-ph/0407232)
- Laor, A. 2001, *ApJ*, 553, 677
- Magorrian, J., et al. 1998, *AJ*, 115, 2285
- Mao, S., Witt, H.J., & Koopmans, L.V.E. 2001, *MNRAS*, 323, 301
- McLure, R.J., & Dunlop, J.S. 2001, *MNRAS*, 327, 199
- McLure, R.J., & Dunlop, J.S. 2002, *MNRAS*, 331, 795
- Monaco, P., Salucci, P., & Danese, L. 2000, *MNRAS*, 311, 279
- Peterson, B.M., et al. 2004, *ApJ*, 613, 682
- Ravindranath, S., Ho, L.C., Peng, C.Y., Filippenko, A.V., & Sargent, W.L.W. 2001, *AJ*, 122, 653
- Robertson, B., Hernquist, L., Cox, T.J., Di Matteo, T., Hopkins, P.F., Martini, P., & Springel, V. 2005, *ApJ*, submitted (astro-ph/0506038)
- Rusin, D., & Ma, C.-P. 2001, *ApJL*, 549, L33
- Rusin, D., Kochanek, C.S., & Keeton, C.R. 2003, *ApJ*, 595, 29

- Rusin, D., & Kochanek, C.S. 2005, *ApJ*, 623, 666
- Schneider, P. 1985, *A&A*, 143, 413
- Tremaine, S., et al. 2002, *ApJ*, 574, 740
- Treu, T., & Koopmans, L.V.E. 2004, *ApJ*, 611, 739
- Treu, T., Malkan, M.A., & Blandford, R.D. 2004, *ApJL*, 615, L97
- Trujillo, I., Erwin, P., Asensio Ramos, A., & Graham, A.W. 2004, *AJ*, 127, 1917
- Wallington, S., & Narayan, R. 1993, *ApJ*, 403, 517
- Winn, J.N., Hall, P.B., & Schechter, P.L. 2003a, *ApJ*, 597, 672
- Winn, J.N., Rusin, D., & Kochanek, C.S. 2003b, *ApJ*, 587, 80
- Winn, J.N., Rusin, D., & Kochanek, C.S. 2004, *Nature*, 427, 613
- Wyithe, J.S.B., & Loeb, A. 2002, *ApJ*, 581, 886

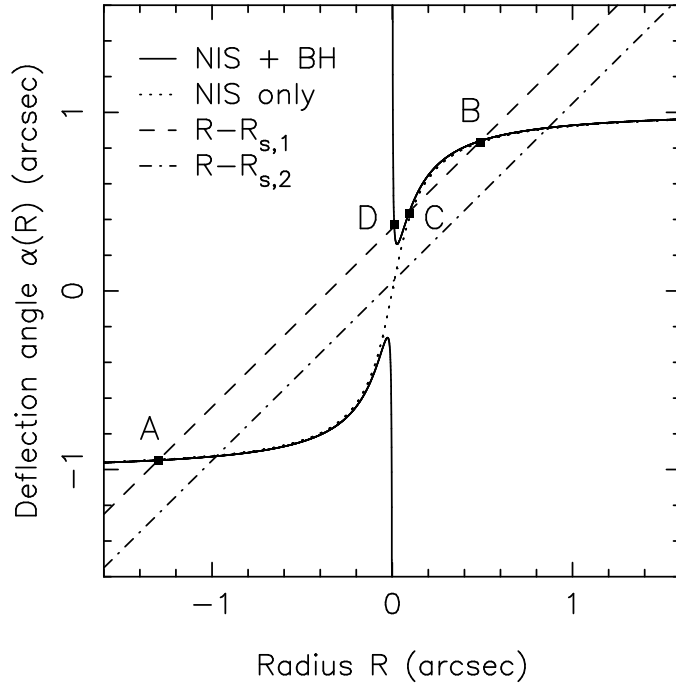


Fig. 1.— Phenomenology of central images, as illustrated by a NIS model. We plot the deflection profile $\alpha(R)$ with (solid line) and without (dotted line) a central black hole. Intersections of $\alpha(R)$ and the line $R - R_s$ (where R_s is the source-plane radius) mark the locations of lensed images. The NIS alone produces three images (A, B, C) of any source within the radial caustic. In the presence of a central black hole, a fourth image (D) is produced for sufficiently misaligned sources ($R_{s,1}$: dashed line), while for well-aligned sources image C is destroyed ($R_{s,2}$: dash-dotted line).

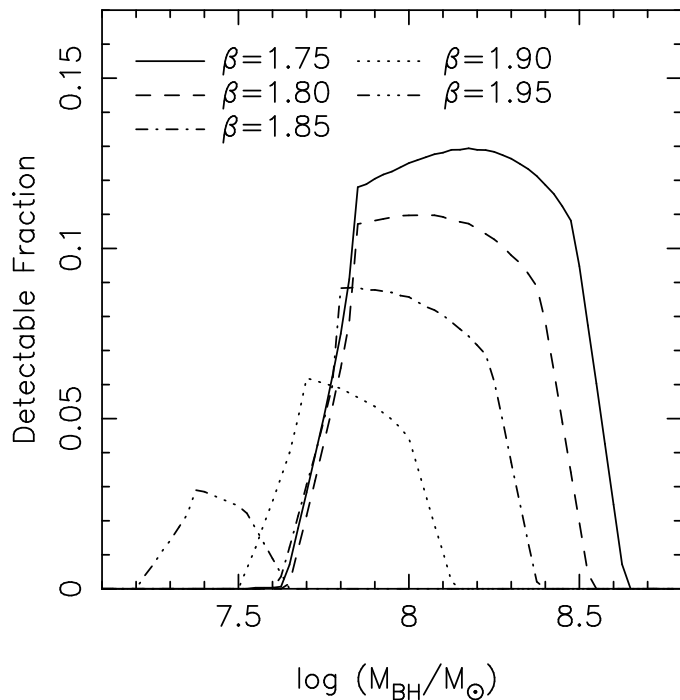


Fig. 2.— Detectability of central image pairs produced by a PL galaxy with a supermassive black hole. We plot the fraction of source positions inside the radial caustic that satisfy image magnification ratio cuts of $\mu_C/\mu_A > 2 \times 10^{-3}$ and $\mu_D/\mu_C > 10^{-2}$. The lens redshift is 0.5, the source redshift is 1.5, and the Einstein radius is $0''.75$ for these and all subsequent simulations. We show results for five different profile slopes, spanning the range $1.75 \leq \beta \leq 1.95$. According to the local $M_{BH}-\sigma$ relation, the model galaxy should host a SMBH with $\log(M_{BH}/M_\odot) = 8.2 \pm 0.2$.

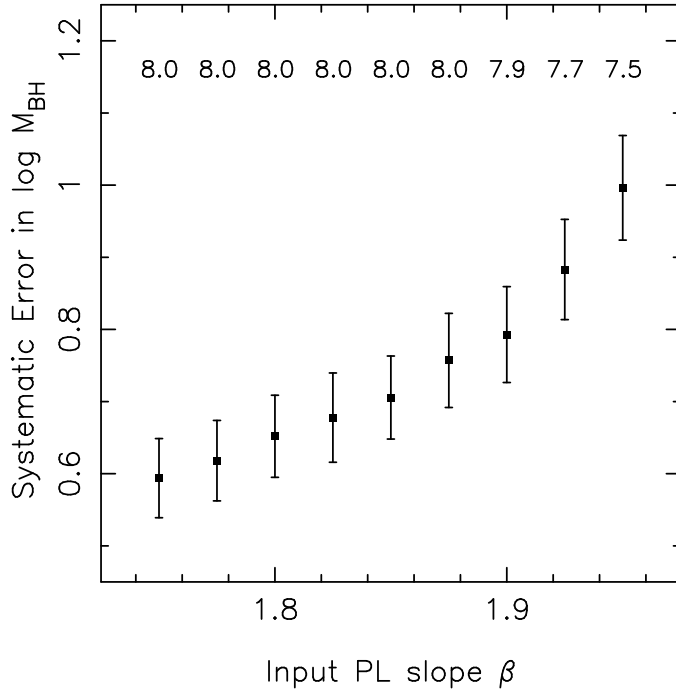


Fig. 3.— Systematic errors in black hole mass measurement. For each input PL slope β , simulated lenses are created using a representative black hole mass [note the values of $\log(M_{BH}/M_{\odot})$ listed above the data points] that produces detectable central images. These lenses are then fitted with a NIS model. We plot the difference between the mean recovered value of $\log M_{BH}$ from the NIS model, and the input $\log M_{BH}$. Values of M_{BH} extracted using the NIS are systematically larger than the PL values by 0.6–1.0 dex. The dependence of the systematic offset on M_{BH} at fixed β is not plotted, but it is a weak function, varying by less than 0.1 dex over the entire range of M_{BH} that produces detectable central images. Moreover, the systematic offset is not sensitive to the magnification cuts applied to the simulated lens sample.

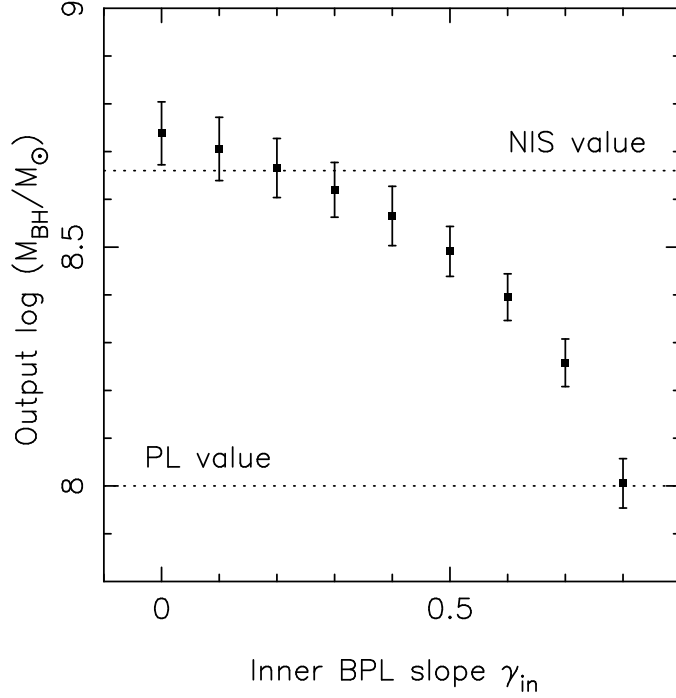


Fig. 4.— Systematic errors related to the inner profile slope. Simulated lens systems, created from a PL mass distribution with slope $\beta = 1.80$ and $\log(M_{BH}/M_{\odot}) = 8.0$ (representative choices), are fitted with a BPL surface density model with outer slope $\gamma_{out} = 1$. We plot the mean value of $\log M_{BH}$ extracted from the BPL fit, and find that it varies systematically with the inner BPL slope γ_{in} . Also shown are the input $\log M_{BH}$, and the mean value extracted from a fit using a NIS, which can be approximated by a BPL with $\gamma_{in} = 0$.